ACS OMEGA

Article

Cite This: ACS Omega 2019, 4, 2750−2757

http://pubs.acs.org/journal/acsodf

Simple and Affordable Way To Achieve Polymeric Superhydrophobic Surfaces with Biomimetic Hierarchical Roughness

Jingyao Sun,[†] Hanwen Li,[†] Yao Huang,[†] Xiuting Zheng,[†] Ying Liu,[‡] Jian Zhuang,*[,†] and Daming Wu*[,†,‡]

[†]College of Mechanical and Electrical Engineering, Beijing University of Chemical Technology, Beijing 100029, China

[‡]State Key Laboratory of Organic-Inorganic Composites, Beijing 100029, China

ABSTRACT: A water contact angle greater than 150° together with a sliding angle less than 10° is a special surface phenomenon that appears on superhydrophobic surfaces. In this paper, a brief introduction of the development history and present research on superhydrophobic surfaces was given. Polymeric superhydrophobic surfaces with biomimetic hierarchical roughness were fabricated by a simple method of hot embossing without any chemical treatments. Stainless steel meshes with different mesh numbers were used as template. Moreover, the influences of processing parameters, including mesh number, mold temperature, and pressure, were deeply investigated. Hierarchical microplatforms, microfibers, and oriented arrayed nanowrinkles structure on them, which were resembled with the nanowrinkles structure and hierarchical roughness on a red rose petal, were observed by a scanning electron microscope. A water contact angle of 154° can be achieved after parameter optimization. The method proposed in this study offered a fine and affordable choice for the fabrication of polymeric superhydrophobic surfaces. With the rapid development of functional applications in micro- and nanodevices, this method will show greater superiority in large-area and large-scale production due to its advantages of low cost, high efficiency, and high reliability.

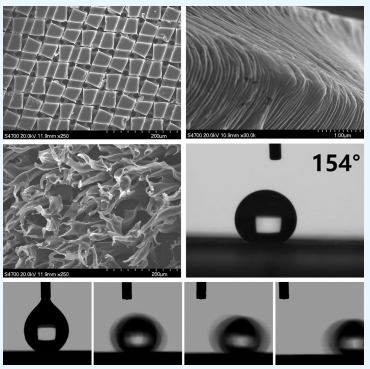

1. INTRODUCTION

Compared with the pioneer research work around the turn of the century,[1−3] the fabrication and fundamental of superhydrophobic surfaces have been extensively studied in recent years.[4−8] Superhydrophobic surfaces are typically defined as surfaces with contact angles of water droplets greater than 150° and sliding angles less than 10°. This rapid expansion of research interest is because of their great application potential in the area of rain, snow, or ice adhesion prevention;[9,10] drag reduction;[11] antibiofouling;[12,13] tunable isotropic or anisotropic wettability surfaces;[14−16] etc. The research of superhydrophobic surfaces is often inspired by natural examples, such as the water repellency and self-cleaning effect of plant leaves and insect wings.[17−21] One of the most well-known examples is the so-called "lotus effect", which can realize self-cleaning using rolling water drops to remove pollutants and dust.[22,23] Basing on the research on natural superhydrophobic phenomenon, artificial superhydrophobic surface was more controllable under the combination of low-surface-energy materials or coatings and designed hierarchical roughness on both micro- and nanoscales.[24−26] Numerous methods for artificial superhydrophobic surfaces fabrication, including chemical composition control and fabrication techniques, such as self-assembly,[27,28] spin coating,[29] electrospinning,[30] etching,[31] imprint lithography,[32] etc., have been developed to reduce surface energy and generate hierarchical roughness.[2,33−36]

Hierarchical roughness is a catch-all for all types of combined structure ranging from microscale to nanoscale.[37] Numerous kinds of hierarchical structures, both natural and artificial, are conducive to the increase of contact angle toward superhydrophobic surfaces. Among the fabricating techniques listed above, imprint lithography is often used in the preparation of superhydrophobic surfaces with hierarchical structures because of its high precision, high fidelity, and simplicity.[20,38] Liu et al. reported an imprint lithography approach to transfer complex micro/nanostructures into polymeric materials with an aluminum oxide mold.[39] Lee's group prepared overhang structures using reverse nanoimprint lithography with poly(vinyl alcohol) transfer template. A fluoroalkylsilane monolayer coating was further performed to reduce the surface energy to form superhydrophobic surfaces on silicon substrates.[40] Many biomimetic hierarchical structures, such as red rose petal, butterfly wing, gecko foot, and plant leaf structures,[41,42] have also been replicated by imprint lithography with either natural material or artificially patterned molds.

Beyond ordered hierarchical structures, the spontaneous surface wrinkling technique[43,44] developed in recent years provides an alternative way to create textured structures on

Received: November 9, 2018
Accepted: January 21, 2019
Published: February 6, 2019

DOI: 10.1021/acsomega.8b03138
ACS Omega 2019, 4, 2750−2757

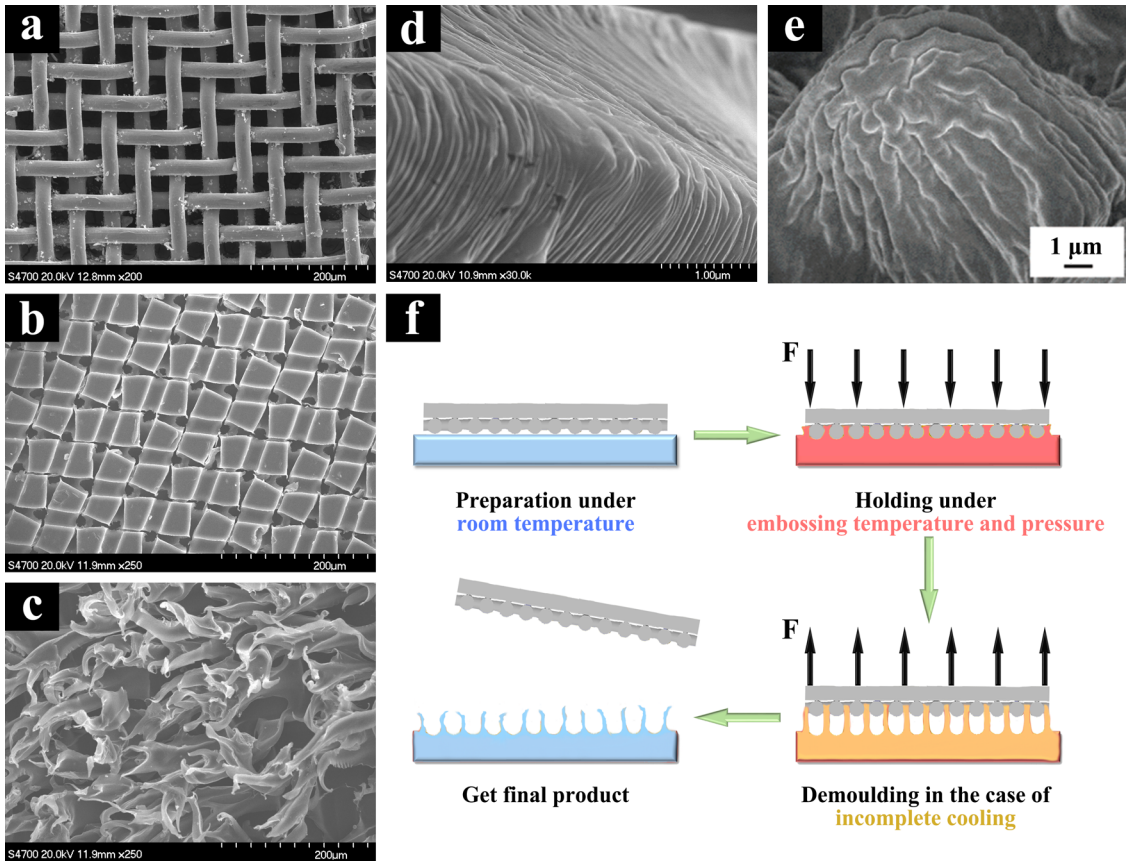

Figure 1. (a) SEM image of the pristine stainless steel mesh with a mesh number of 300; (b, c) the as-prepared surfaces using same template showing totally different morphologies under varying processing parameters; (d) regularly arranged nanowrinkles on microfiber structures; (e) SEM image of the nanowrinkles on red rose petal; and (f) the formation and evolution process of the special biomimetic hierarchical structures.

both micro- and nanoscales. Researchers around the world have made many efforts to fabricate hierarchical wrinkle and fold structures for the realization of controllable wetting characteristics. To date, external stress or strain under appropriate conditions is considered to be an effective way to fabricate hierarchically wrinkled surfaces.[45] Some other techniques such as plasma treatment, thermally induced shrinkage, and imprint lithography are also applied combining with spontaneous wrinkling for better controllability. Lee et al.[46] transformed flat polystyrene substrates into superhydrophobic hierarchically wrinkled surfaces by sequential wrinkling process. Plasma treatments followed by directional strain relief were performed to control the nanowrinkle orientation and wavelength. Zhang et al.[47] explored the formation mechanism of hierarchically wrinkled surfaces, which can be controlled between superhydrophobicity and superhydrophilicity by mechanical strain. The relationship between different contact states and levels of hierarchical roughness was also discussed. Moreover, superhydrophobic surfaces with hierarchical roughness, such as combinations of wrinkles with micropillars, microplatforms, microfibers, etc., have been successfully fabricated and comprehensively studied.[48−50]

Although the aforementioned techniques could generate superhydrophobic surfaces with hierarchical roughness, the preparation of hierarchically structured superhydrophobic products still cannot meet the demands of large-scale industrialization (e.g., efficiently, massively, and cheaply). Therefore, it is worthwhile to develop efficient, controllable, and affordable techniques to fabricate optimized hierarchically structured surfaces and further promote the research depth on their hydrophobic characteristics.

In this paper, we select the hot embossing method, which can be regarded as a special type of imprint lithography, to fabricate polymeric superhydrophobic surfaces with biomimetic hierarchical structures. Hierarchical microplatforms, microfibers, and oriented arrayed nanowrinkles structures, which are similar to the wrinkled surfaces of red rose petal, are generated on polymer substrates under precisely controlled temperature and pressure. As a kind of top-down approach, the hot embossing method has the advantages of easy handling, high efficiency, high fidelity, and low cost.[51,52] Extra large (>feet^2) products with superior hydrophobic performance can be obtained within 1 min with no chemical treatment. The application of commercial polymer substrate and stainless steel mesh template makes the fabrication of superhydrophobic surfaces really repeatable and affordable. The size of products with biomimetic hierarchical roughness can be even larger when larger polymer substrate, mesh template, and hot embossing equipment are used. Therefore, this method is ideal for mass industrial production of polymeric superhydrophobic surfaces.

2. RESULTS AND DISCUSSION

2.1. Formation and Evolution of the Biomimetic Hierarchical Roughness. The surface morphology of final product was determined by the combination of stainless steel mesh and the processing parameters of hot embossing. The

DOI: 10.1021/acsomega.8b03138
ACS Omega 2019, 4, 2750−2757

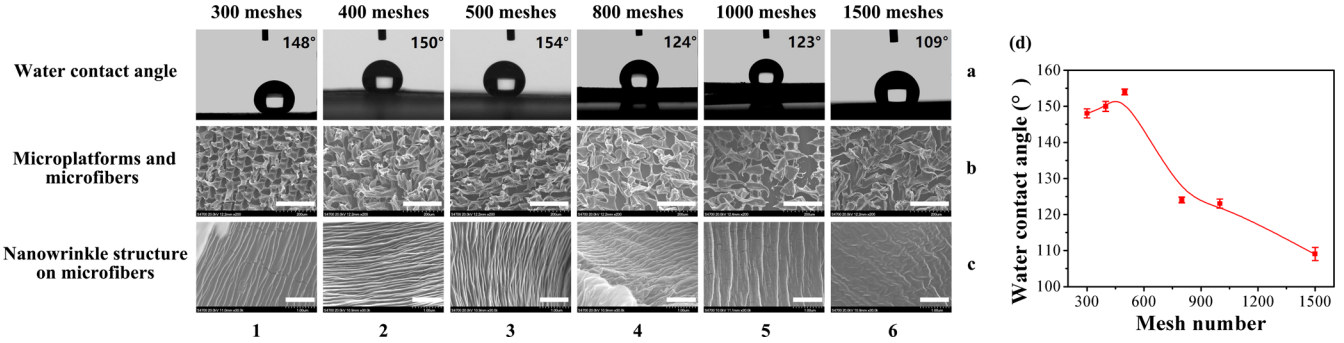

Figure 2. (a) Water contact angles and morphologies on (b) microscale and (c) nanoscale of the as-prepared samples using stainless steel meshes with different mesh numbers as templates. (d) Relationship between mesh number and hydrophobic performance of the as-prepared samples. The scale bars in the insets of (b) and (c) are 200 and 1 μm, respectively.

diameter of the wire mesh and mesh size, which are influenced by the mesh number, would directly affect the size of the microplatform structure in final product. Meanwhile, the processing parameters (e.g., embossing temperature and pressure) would greatly influence the formation and evolution of microfiber and nanowrinkle structures. The specifications of stainless steel mesh had already been standardized. Here, meshes with mesh numbers of 300, 400, 500, 800, 1000, and 1500 were selected for hot embossing experiments. Figure 1a shows the scanning electron microscopy (SEM) image of the pristine stainless steel mesh with a mesh number of 300.

Two SEM images of the as-prepared surfaces using same template are presented in Figure 1b,c. Although the template of these two samples was the same, different processing parameters, especially different embossing temperatures, led to totally different morphological characteristics. When the embossing temperature was lower than the melting temperature (T_m) of ethylene vinyl acetate (EVA) and polyethylene (PE), the structure of the surface was mainly microplatforms, which were basically of the same size with the meshes (as shown in Figure 1b). The microplatform structures can be regarded as notches of the stainless steel meshes on polymer substrates caused by mechanical compression and embedding. With the increase of embossing temperature, polymer substrate (especially the EVA phase) would have stronger deformability and mobility, which led to total variation of the microplatform structures. Figure 1c presents the morphology of sample prepared under embossing temperature several degrees higher than in Figure 1b. Obviously, almost all of the microplatforms changed into microfibers. More details on the surface of microfibers can be found under higher magnification (30 K). As shown in Figure 1d, nanowrinkle array with a cycle of ∼100 nm, which was very similar to the nanowrinkle structures on red rose petal (Figure 1e), was regularly arranged along the axial direction of microfiber. The nanowrinkles together with microplatforms and microfibers formed by the hot embossing process constituted the needed hierarchical roughness for superhydrophobic surfaces. The formation and evolution process of this special biomimetic hierarchical structure is revealed in Figure 1f. First, the stainless steel mesh and PE substrate were prepared under room temperature and then put into the hot embossing device together. Second, they were embossed and held for a certain time under predefined embossing temperature and pressure. During this step, the mesh would be gradually pressed into PE substrate and the morphology should be similar to the one presented in Figure 1b. After that, the demolding step (peeling the mesh off PE substrate) was performed immediately in the case of incomplete cooling. To get perfect microfibers and nanowrinkles on them, the embossing temperature should be set at certain values that are slightly higher than the T_m of EVA and lower than the T_m of PE. On account of the strong deformability and mobility of melting EVA, the gaps of stainless steel mesh could be fully filled, and the polymer (both EVA and PE) attached on net wires would be stretched and turned into the microfibers in Figure 1c, while unmelted PE phase held the whole substrate together and kept it from falling apart. During the stretching process, the surface layer (outer layer) of the formed microfibers was cooled down rapidly by air; however, the temperature of the inner layer still kept at a high level. Thus, different deformabilities between the outer and inner layers of microfibers would lead to continuous melt fracture phenomenon and form the axially arranged nanowrinkles in Figure 1d. The final morphology of nanowrinkles was also significantly influenced by the nonuniform shrinkage and creep after fracture of microfibers or detaching from net wires. In this way, superhydrophobic surfaces with biomimetic hierarchical roughness were finally obtained. The whole hot embossing process can be done within 20 s, representing a relatively high efficiency for the preparation of superhydrophobic surfaces.

Although many researchers had reported their methods for the preparation of biomimetic nanowrinkles and hierarchical roughness, the method we proposed in this paper was undoubtedly one of the most efficient and affordable ones. All our method required was a piece of commercialized screen mesh, polymer substrates, and suitable temperature and pressure conditions. No chemical treatment and expensive equipment were needed.

2.2. Influence of Different Parameters on Surface Morphology and Hydrophobic Performance. Different parameters, especially mesh number, embossing temperature, and pressure, had significant impacts on the surface morphology and hydrophobic performance of final products. In this section, their influences will be investigated and discussed systematically to find out the optimal processing parameters. Furthermore, the relationship between surface morphology and hydrophobic performance will also be explored.

Figure 2 shows the influence of templates (stainless steel meshes with different mesh numbers) on surface morphology and hydrophobic performance of the as-prepared samples. In this figure, (a)−(c) represent the characterization results of water contact angle and morphologies on micro- and

DOI: 10.1021/acsomega.8b03138
ACS Omega 2019, 4, 2750−2757

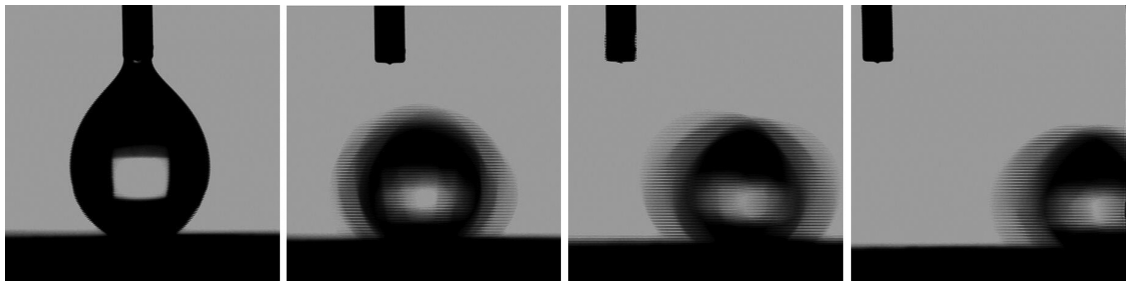

Figure 3. Water droplet rolling on the as-prepared PE surface tilted ~1°.

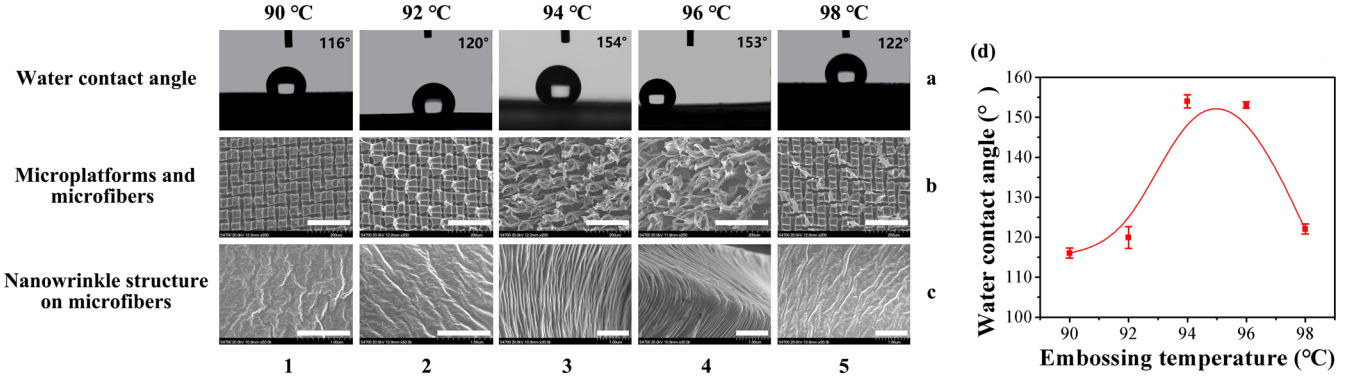

Figure 4. (a) Water contact angles, and morphologies on (b) microscale and (c) nanoscale of samples prepared by isothermal hot embossing with different embossing temperatures. (d) Relationship between embossing temperature and hydrophobic performance of the as-prepared samples. The scale bars in the insets of (b) and (c) are 200 and 1 μm, respectively.

nanoscales, while 1−6 denote the variation of mesh numbers from 300 to 1500. Therefore, Figure 2a1 here represents the water contact angle of the as-prepared sample using stainless steel mesh with a mesh number of 300 as template. Similarly, the SEM image named Figure 2b2 represented the sample morphology on microscale (microplatforms and microfibers) using stainless steel mesh with a mesh number of 400 as template, and Figure 2c3 represents the sample morphology on nanoscale (regularly arranged nanowrinkles on microfibers) using stainless steel mesh with a mesh number of 500 as template. The rest of the pictures can be named and explained in the same manner.

The embossing temperature and pressure for all of the as-prepared samples presented in Figure 2 were 94 °C and 6 MPa, respectively. According to the measurement results, the contact angle of untreated PE/EVA composite substrates was ~93°, whereas that of the as-prepared samples had been enlarged in different degrees (as shown in Figure 2d). The contact angle of the as-prepared sample using stainless steel mesh with a mesh number of 300 as templates was 148°. This contact angle would increase with increasing mesh number and reach a maximum of 154° when the mesh number was 500. After that, further increase of mesh number will lead to opposite effects and sharply reduce the contact angle to around 109° (mesh number = 1500). The increase of contact angle in the first stage was attributed to the size reduction of microstructures on PE/EVA substrate, which was determined by the decreasing mesh size with larger mesh numbers. Based on the Wenzel−Cassie model, the increase of surface roughness was beneficial to enhance the hydrophobic characteristic of the as-prepared samples, while higher surface roughness can raise the proportion of air phase in solid−liquid−air interface. Larger mesh number would lead to higher surface roughness during the hot embossing process (as shown in Figure 2b1−b3) before the mesh number reached 500. Higher surface roughness would keep more air bubbles (on both micro- and nanoscales) when water droplets dropped onto polymer surfaces. The wetting of areas under air bubbles, especially the wetting of bubbles between each nanowrinkle, was extremely difficult owing to the effect of surface tension. Further, the dense air bubbles within hierarchical structures would form a layer of air cushion between water droplet and polymer surface, which finally created a polymeric superhydrophobic surface with durable performance. In Figure 2b3, the most compact microfiber structure was obtained. Further, oriented arranged nanowrinkle structures could be observed on the surface of microfibers in each sample at much higher magnification (30 000×). Compact nanowrinkles with higher amplitudes were available when the mesh numbers were 400 and 500 (as shown in Figure 2c2,2c3, respectively). The combination of compact microfibers and convex nanowrinkles on them ultimately led to superior hydrophobicity of the as-prepared sample in Figure 2a2,a3 (150 and 154°, respectively). Then, in the second stage, further increase of the mesh number would lead to decline of contact angle. In most cases, when the mesh number was higher than 500, the whole stainless steel mesh would be composed by several layers (with lower mesh number) to reduce the relative size of the aperture. The overlap between different layers would increase the entering difficulty of melting polymer and show negative effects on the formation of hierarchical roughness. As shown in Figure 2b4−b6, the size of microstructures on PE/EVA substrates did not decrease but became more messy and irregular with the increase of mesh number above 500. The amplitude and compactness of nanowrinkles in Figure 2c4−c6 also presented obvious downtrends.

DOI: 10.1021/acsomega.8b03138
ACS Omega 2019, 4, 2750−2757

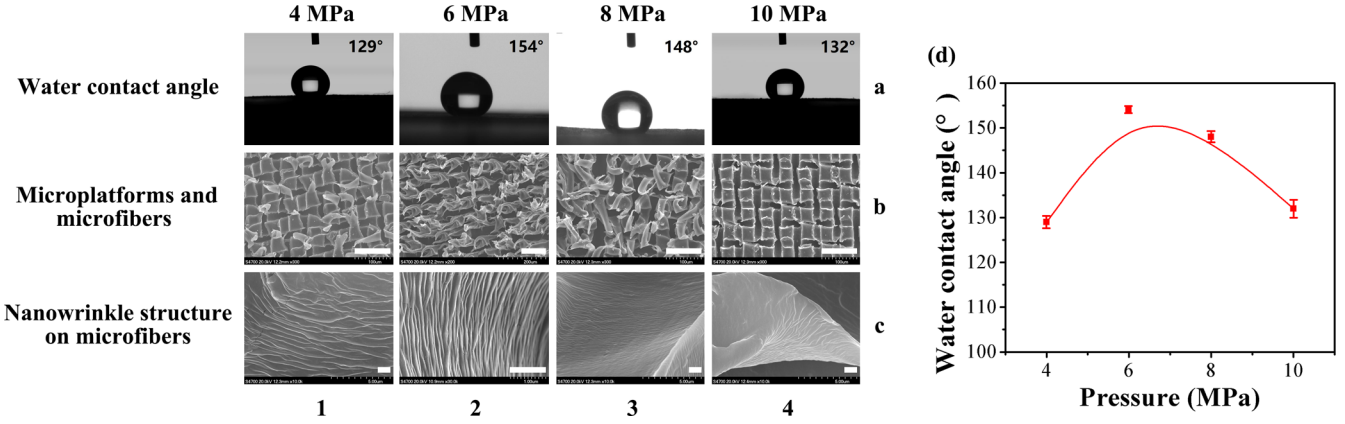

Figure 5. (a) Water contact angles, and morphologies on (b) microscale and (c) nanoscale of samples prepared by isothermal hot embossing with different pressures. (d) Relationship between pressure and hydrophobic performance of the as-prepared samples. The scale bars in the insets of (b) and (c) are 100 and 1 μm, respectively.

Furthermore, the water adhesion of the surface with a contact angle of 154° was investigated by droplet rolling test. A 10 μL water droplet was suspended from a microsyringe in air. Figure 3 shows that the water droplet readily rolled on the as-prepared surface tilted ∼1°, which indicated that the water sliding angle was extremely low. Thus, comprehensive analysis of the results of water contact angle, sliding angle, and SEM image was conducted, and the optimal mesh number of the template used for the preparation of superhydrophobic surfaces with biomimetic hierarchical roughness should be around 500.

After confirming the optimal mesh number for templates, further investigation on the influence of embossing temperature on surface morphology and hydrophobic performance was carried out. The mesh number of template and pressure for all of the as-prepared samples presented in Figure 4 were 500 and 6 MPa, respectively. When the embossing temperature was just reached or lower than 92 °C, rare microfibers can be found after embossing (as shown in Figure 4b1,b2) according to the poor deformability. Similarly, the formation of nanowrinkles was also restricted by the limited deformability, which led to irregular arrangement and low amplitude of nanowrinkles (Figure 4c1,c2). As mentioned above, the biomimetic hierarchical roughness was composed of microplatforms, microfibers, and nanowrinkles, and undesirable combinations of the micro- and nanostructures eventually led to poor hydrophobicity (116 and 120° in Figure 4a1,a2, respectively). After the embossing temperature rose up to around or above T_m of EVA, normally formed microplatforms, dense microfibers (Figure 4b3,b4) with a length of ∼100 μm and compact convex nanowrinkles (Figure 4c3,c4) with relatively high amplitude (ca. 100−150 nm) together constituted the perfect hierarchical roughness and sharply rose the water contact angle up to more than 150°. The contact angles of the as-prepared samples with embossing temperatures of 94 and 96 °C were 154 and 153° (Figure 4a3,a4), respectively. That is, 94−96 °C can be recognized as the optimal range of embossing temperature for the preparation of superhydrophobic surfaces with hierarchical roughness. However, the optimal range of embossing temperature was so narrow that further increase would lead to undesirable morphologies (Figure 4b5,c5) and sharp reduction of contact angle (122° in Figure 4a5).

A similar research process was also applied to find the optimal pressure. Figure 5 presents the results of water contact angle and morphology of the as-prepared samples. The mesh number of template and embossing temperature applied in the hot embossing process were 500 and 94 °C, respectively. As shown in Figure 5d, the optimal pressure was around 6 MPa and the water contact angle can be higher than 150° (Figure 5a2). The most important influence factor in this experimental group was the forming results of microplatforms and microfibers on account of the same temperature condition and the consequent same forming ability of nanowrinkles. Thus, although the forming results of nanowrinkles in Figure 5c1 were good enough, the hydrophobicity of the corresponding samples was not that good (129° in Figure 5a1) due to the sparse microfibers (as shown in Figure 5b1) and the consequent imperfect hierarchical roughness. This could also explain the undesirable hydrophobicity of the as-prepared samples fabricated with 10 MPa pressure (132° in Figure 5a4). Majority of the microfibers would be snapped during the demolding step as too much melting polymer went through the template under such high pressure and formed a "mushroom-like" structure during the embossing step.

Overall, the optimal processing parameters for the preparation of PE/EVA superhydrophobic surfaces with biomimetic hierarchical roughness should be 94 °C and 6 MPa. The best templates were stainless steel meshes with a mesh number of 500. In this way, perfect biomimetic hierarchical roughness can be obtained, and the whole preparation cycle of isothermal hot embossing can be as short as 20 s. With the advantages of low equipment requirement and easy operation of isothermal hot embossing, the preparation method proposed in this paper was doubtlessly a simple and affordable way to achieve polymeric superhydrophobic surfaces. Furthermore, it also showed greater superiority in large-area and large-scale production due to its advantages of low cost, high efficiency, and high reliability.

Besides hydrophobicity, the lipophobicities of the as-prepared samples before and after hot embossing were also measured and compared to demonstrate the promoting effect of biomimetic hierarchical roughness on wettability. Since the surface tension of oil was lower than that of water, the promotion of lipophobicity was much harder than that of hydrophobicity. As shown in Figure 6a,b, water contact angles of the as-prepared samples before and after isothermal hot

DOI: 10.1021/acsomega.8b03138
ACS Omega 2019, 4, 2750−2757

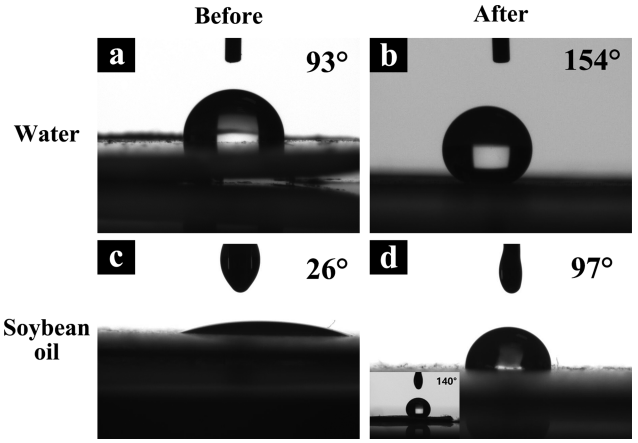

Figure 6. Comparison of (a, b) hydrophobicity and (c, d) lipophobicity of PE samples before and after hot embossing. The inset presents the lipophobicity of PE sample after hot embossing and fluorosilane modification.

embossing under the aforementioned optimal parameters were 93 and 154°, respectively. However, the oil contact angles of the same samples were 26 and 97°, respectively (Figure 6c,d). Although the promotion of oil contact angles from 26 to 97° was an obvious one, it still cannot meet the usage requirements in most situations (e.g., self-cleaning and antioil). A much higher oil contact angle of 140° can be obtained after modifying the PE/EVA surface with fluorosilane (as shown in the inset of Figure 6d). The hierarchical roughness and low surface energy of modified samples had worked together to create the significant promotion of oil contact angle from 26 to 140°.

3. CONCLUSIONS

In this paper, stainless steel meshes were applied as templates for the preparation of polymeric superhydrophobic surfaces with biomimetic hierarchical roughness via isothermal hot embossing. Herein, the hierarchical roughness was composed of microplatforms, microfibers, and oriented arrayed nanowrinkles formed during the demolding step. After parameter optimization, the optimal processing parameters for PE/EVA samples prepared by the hot embossing method were decided to be 94 °C and 6 MPa, while the best templates were stainless steel meshes with a mesh number of 500. A water contact angle of 154° and an oil contact angle of 97° can be achieved under the aforementioned optimal parameters. After further modifying using fluorosilane, the oil contact angle would increase to 140° under the cooperation of hierarchical roughness and low surface energy. In addition, water droplets were found to roll readily on the as-prepared surface tilted ∼1°, which indicated an extremely low water sliding angle. It was worth mentioning that the whole hot embossing process can be finished within 20 s, and this method was also suitable for extra large (>feet^2) samples. By changing the size of polymer substrate, mesh template, and hot embossing equipment, superhydrophobic surfaces with biomimetic hierarchical roughness can be even larger. Therefore, the method proposed in this paper was a simple and affordable way for the mass industrial production of polymeric superhydrophobic surfaces.

4. EXPERIMENTAL SECTION

4.1. Materials and Experimental Devices. Stainless steel meshes with different mesh numbers (Shanghai Yixiang stainless steel screen mesh manufacturer, China) were used as templates in the preparing process. Polyethylene/ethylene vinyl acetate (PE/EVA) copolymer composite substrates with a thickness of 0.3 mm were purchased from Dongguan Ruihang Plastic Materials Co., Ltd. The specific components of this composite substrate were evaluated by differential scanning calorimetry (DSC).[53] As shown in Figure 7, three

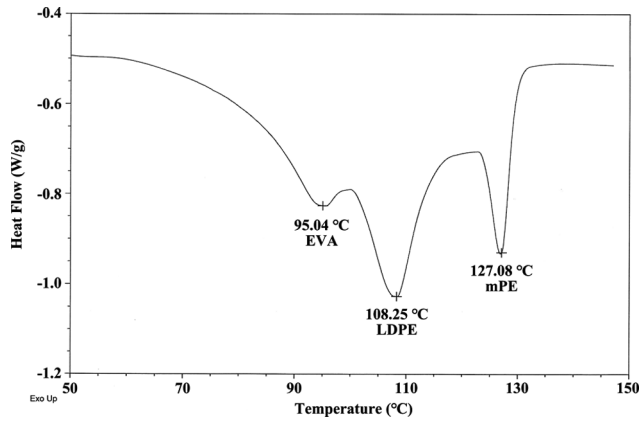

Figure 7. Differential scanning calorimeter (DSC) melting curve at 10 K min^{-1} (typical sample mass, 5 mg).

absorption peaks at 95.04, 108.25, and 127.08 °C can be observed on the DSC melting curve, representing EVA, low-density polyethylene, and metallocene polyethylene, respectively. Transparent polycarbonate (PC) substrates with a thickness of 0.25 mm were provided by Dongguan Lingmei New Materials Co., Ltd. for use as supports during hot embossing. A homemade hot embossing device, which can provide precisely controlled embossing temperature and pressure, was utilized to perform the plate-to-plate isothermal hot embossing for the preparation of superhydrophobic surfaces. The plate-to-plate isothermal hot embossing process was ideal for large-scale production of functional microdevice with pretty high efficiency down to 20 s. The most important feature of isothermal hot embossing was its constant and relatively low mold temperature during the whole embossing process.

4.2. Preparation of Polymeric Superhydrophobic Surfaces. First, PE/EVA substrates and stainless steel meshes were cut into appropriate size (90 × 60 mm^2) and then wiped clean using absolute alcohol for further applications. Here, the product size can be even larger as the only limitation was the size of the experimental platform. Second, a small amount of demolding agent was sprayed on the surfaces of PE/EVA substrate and stainless steel mesh for easier demolding. Third, the PE/EVA substrate (at the bottom) and stainless steel mesh (on top) were placed together in the embossing area of the experimental device. Two pieces of PC substrates were also placed on their both sides as supports. Precisely controlled temperature and pressure were set for isothermal hot embossing. The "isothermal" indicated the constant embossing temperature in the whole process, which will significantly reduce the cycle time from more than 10 min to ∼20 s.[51,52,54,55] After embossed for a certain holding time and demolding process (quickly peeling off from the stainless steel

DOI: 10.1021/acsomega.8b03138
ACS Omega 2019, 4, 2750−2757

mesh in the case of incomplete cooling), PE/EVA substrate with superhydrophobic performance was finally obtained. And it is worth mentioning that the hot embossing method for the preparation of micro/nanostructures and hierarchical structures can be applied for other thermoplastic polymers, such as PC, polymethyl methacrylate, polypropylene, and so on. The structure type is also designable depending on different materials, situations, and applications.[21,54,56]

4.3. Characterization. The morphology of fabricated surface with hierarchical roughness was observed by a field emission scanning electron microscope (S-4700, Hitachi, Japan).[57,58] The contact angles of water droplets of the as-prepared samples were measured by a drop shape analyzer (DSA100, KRÜSS, Germany). Soybean oil was used for measuring and comparing oil contact angles.

AUTHOR INFORMATION

Corresponding Authors

*E-mail: vipzhuangjian@163.com (J.Z.).
*E-mail: wudaming@vip.163.com Tel: +86-10-64435015. Fax: +86-10-64435015 (D.W.).

ORCID

Jingyao Sun: 0000-0002-0140-0212

Notes

The authors declare no competing financial interest.

ACKNOWLEDGMENTS

The authors acknowledge the financial support by the National Natural Science Foundation of China (Nos. 51673020 and 51173015).

REFERENCES

(1) Nakajima, A.; Fujishima, A.; Hashimoto, K.; Watanabe, T. Preparation of Transparent Superhydrophobic Boehmite and Silica Films by Sublimation of Aluminum Acetylacetonate. *Adv. Mater.* **1999**, *11*, 1365−1368.

(2) Erbil, H. Y.; Demirel, A. L.; Avci, Y.; Mert, O. Transformation of a simple plastic into a superhydrophobic surface. *Science* **2003**, *299*, 1377−80.

(3) Jiang, L.; Zhao, Y.; Zhai, J. A Lotus-Leaf-like Superhydrophobic Surface: A Porous Microsphere/Nanofiber Composite Film Prepared by Electrohydrodynamics. *Angew. Chem.* **2004**, *116*, 4438−4441.

(4) Guo, Z.; Liu, W.; Su, B.-L. Superhydrophobic surfaces: From natural to biomimetic to functional. *J. Colloid Interface Sci.* **2011**, *353*, 335−355.

(5) Liu, Y.; Moevius, L.; Xu, X.; Qian, T.; Yeomans, J. M.; Wang, Z. Pancake bouncing on superhydrophobic surfaces. *Nat. Phys.* **2014**, *10*, 515−519.

(6) Tian, X.; Verho, T.; Ras, R. H. A. Moving superhydrophobic surfaces toward real-world applications. *Science* **2016**, *352*, 142−143.

(7) Schellenberger, F.; Encinas, N.; Vollmer, D.; Butt, H.-J. How Water Advances on Superhydrophobic Surfaces. *Phys. Rev. Lett.* **2016**, *116*, No. 096101.

(8) Sohn, E. H.; Kang, H. S.; Bom, J.-C.; Ha, J.-W.; Lee, S.-B.; Park, I. J. Silica-Core Perfluorinated Polymer-Shell Composite Nanoparticles for Highly Stable and Efficient Superhydrophobic Surfaces. *J. Mater. Chem. A* **2018**, 12950−12955.

(9) Kim, P.; Wong, T.-S.; Alvarenga, J.; Kreder, M. J.; Adorno-Martinez, W. E.; Aizenberg, J. Liquid-Infused Nanostructured Surfaces with Extreme Anti-Ice and Anti-Frost Performance. *ACS Nano* **2012**, *6*, 6569−6577.

(10) Zhu, H.; Guo, Z.; Liu, W. Adhesion behaviors on superhydrophobic surfaces. *Chem. Commun.* **2014**, *50*, 3900.

(11) Bhushan, B.; Jung, Y. C. Natural and biomimetic artificial surfaces for superhydrophobicity, self-cleaning, low adhesion, and drag reduction. *Prog. Mater. Sci.* **2011**, *56*, 1−108.

(12) Epstein, A. K.; Wong, T. S.; Belisle, R. A.; Boggs, E. M.; Aizenberg, J. Liquid-infused structured surfaces with exceptional anti-biofouling performance. *Proc. Natl. Acad. Sci. U.S.A.* **2012**, *109*, 13182−13187.

(13) Zhang, P.; Lin, L.; Zang, D.; Guo, X.; Liu, M. Designing Bioinspired Anti-Biofouling Surfaces based on a Superwettability Strategy. *Small* **2017**, *13*, No. 1503334.

(14) Sun, W.; Zhou, S.; You, B.; Wu, L. A facile method for the fabrication of superhydrophobic films with multiresponsive and reversibly tunable wettability. *J. Mater. Chem. A* **2013**, *1*, 3146.

(15) Lee, S. G.; Lim, H. S.; Lee, D. Y.; Kwak, D.; Cho, K. Tunable Anisotropic Wettability of Rice Leaf-Like Wavy Surfaces. *Adv. Funct. Mater.* **2013**, *23*, 547−553.

(16) Toma, M.; Loget, G.; Corn, R. M. Flexible Teflon Nanocone Array Surfaces with Tunable Superhydrophobicity for Self-Cleaning and Aqueous Droplet Patterning. *ACS Appl. Mater. Interfaces* **2014**, *6*, 11110−11117.

(17) Liu, K.; Jiang, L. Bio-inspired design of multiscale structures for function integration. *Nano Today* **2011**, *6*, 155−175.

(18) Darmanin, T.; Guittard, F. Superhydrophobic and superoleophobic properties in nature. *Mater. Today* **2015**, *18*, 273−285.

(19) Liu, K.; Yao, X.; Jiang, L. Recent developments in bio-inspired special wettability. *Chem. Soc. Rev.* **2010**, *39*, 3240.

(20) Yan, Y. Y.; Gao, N.; Barthlott, W. Mimicking natural superhydrophobic surfaces and grasping the wetting process: A review on recent progress in preparing superhydrophobic surfaces. *Adv. Colloid Interface Sci.* **2011**, *169*, 80−105.

(21) Sun, J.; Wang, X.; Wu, J.; Jiang, C.; Shen, J.; Cooper, M. A.; Zheng, X.; Liu, Y.; Yang, Z.; Wu, D. Biomimetic Moth-eye Nanofabrication: Enhanced Antireflection with Superior Self-cleaning Characteristic. *Sci. Rep.* **2018**, *8*, No. 5438.

(22) Marmur, A. The Lotus Effect: Superhydrophobicity and Metastability. *Langmuir* **2004**, *20*, 3517−3519.

(23) Cheng, Z.; Du, M.; Lai, H.; Zhang, N.; Sun, K. From petal effect to lotus effect: a facile solution immersion process for the fabrication of super-hydrophobic surfaces with controlled adhesion. *Nanoscale* **2013**, *5*, 2776.

(24) Lee, Y.; Park, S. H.; Kim, K. B.; Lee, J. K. Fabrication of Hierarchical Structures on a Polymer Surface to Mimic Natural Superhydrophobic Surfaces. *Adv. Mater.* **2007**, *19*, 2330−2335.

(25) Gao, X.; Zhou, J.; Du, R.; Xie, Z.; Deng, S.; Liu, R.; Liu, Z.; Zhang, J. Robust Superhydrophobic Foam: A Graphdiyne-Based Hierarchical Architecture for Oil/Water Separation. *Adv. Mater.* **2016**, *28*, 168−173.

(26) Li, Y.; Dai, S.; John, J.; Carter, K. R. Superhydrophobic Surfaces from Hierarchically Structured Wrinkled Polymers. *ACS Appl. Mater. Interfaces* **2013**, *5*, 11066−11073.

(27) Checco, A.; Rahman, A.; Black, C. T. Robust Superhydrophobicity in Large-Area Nanostructured Surfaces Defined by Block-Copolymer Self Assembly. *Adv. Mater.* **2014**, *26*, 886−891.

(28) Rahmawan, Y.; Xu, L.; Yang, S. Self-assembly of nanostructures towards transparent, superhydrophobic surfaces. *J. Mater. Chem. A* **2013**, *1*, 2955−2969.

(29) Xu, L.; Karunakaran, R. G.; Guo, J.; Yang, S. Transparent, superhydrophobic surfaces from one-step spin coating of hydrophobic nanoparticles. *ACS Appl. Mater. Interfaces* **2012**, *4*, 1118−1125.

(30) Nuraje, N.; Khan, W. S.; Lei, Y.; Ceylan, M.; Asmatulu, R. Superhydrophobic electrospun nanofibers. *J. Mater. Chem. A* **2013**, *1*, 1929−1946.

(31) Xue, C.-H.; Li, Y.-R.; Zhang, P.; Ma, J.-Z.; Jia, S.-T. Washable and Wear-Resistant Superhydrophobic Surfaces with Self-Cleaning Property by Chemical Etching of Fibers and Hydrophobization. *ACS Appl. Mater. Interfaces* **2014**, *6*, 10153−10161.

(32) Hensel, R.; Finn, A.; Helbig, R.; Braun, H.-G.; Neinhuis, C.; Fischer, W.-J.; Werner, C. Biologically Inspired Omniphobic Surfaces by Reverse Imprint Lithography. *Adv. Mater.* **2014**, *26*, 2029−2033.

DOI: 10.1021/acsomega.8b03138
ACS Omega 2019, 4, 2750−2757

(33) Zhao, N.; Weng, L.; Zhang, X.; Xie, Q.; Zhang, X.; Xu, J. A Lotus-Leaf-Like Superhydrophobic Surface Prepared by Solvent-Induced Crystallization. *ChemPhysChem* **2006**, *7*, 824−827.
(34) Li, Y.; Chen, S.; Wu, M.; Sun, J. All Spraying Processes for the Fabrication of Robust, Self-Healing, Superhydrophobic Coatings. *Adv. Mater.* **2014**, *26*, 3344−3348.
(35) Sun, J.; Zhao, Y.; Yang, Z.; Shen, J.; Cabrera, E.; Lertola, M. J.; Yang, W.; Zhang, D.; Benatar, A.; Castro, J. M.; et al. Highly stretchable and ultrathin nanopaper composites for epidermal strain sensors. *Nanotechnology* **2018**, *29*, No. 355304.
(36) Sun, J.; Shen, J.; Chen, S.; Cooper, M.; Fu, H.; Wu, D.; Yang, Z. Nanofiller reinforced biodegradable PLA/PHA composites: Current status and future trends. *Polymers* **2018**, *10*, 505.
(37) Guo, L. J. Nanoimprint Lithography: Methods and Material Requirements. *Adv. Mater.* **2007**, *19*, 495−513.
(38) Li, X.-M.; Reinhoudt, D.; Crego-Calama, M. What do we need for a superhydrophobic surface? A review on the recent progress in the preparation of superhydrophobic surfaces. *Chem. Soc. Rev.* **2007**, *36*, 1350.
(39) Liu, X.; Wu, W.; Wang, X.; Luo, Z.; Liang, Y.; Zhou, F. A replication strategy for complex micro/nanostructures with superhydrophobicity and superoleophobicity and high contrast adhesion. *Soft Matter* **2009**, *5*, 3097.
(40) Choi, H.-J.; Choo, S.; Shin, J.-H.; Kim, K.-I.; Lee, H. Fabrication of Superhydrophobic and Oleophobic Surfaces with Overhang Structure by Reverse Nanoimprint Lithography. *J. Phys. Chem. C* **2013**, *117*, 24354−24359.
(41) Jeong, H. E.; Kwak, R.; Khademhosseini, A.; Suh, K. Y. UV-assisted capillary force lithography for engineering biomimetic multiscale hierarchical structures: From lotus leaf to gecko foot hairs. *Nanoscale* **2009**, *1*, 331.
(42) Chang, K.-C.; Lu, H.-I.; Peng, C.-W.; Lai, M.-C.; Hsu, S.-C.; Hsu, M.-H.; Tsai, Y.-K.; Chang, C.-H.; Hung, W.-I.; Wei, Y.; Yeh, J.-M. Nanocasting Technique to Prepare Lotus-leaf-like Superhydrophobic Electroactive Polyimide as Advanced Anticorrosive Coatings. *ACS Appl. Mater. Interfaces* **2013**, *5*, 1460−1467.
(43) Schauer, S.; Worgull, M.; Hölscher, H. Bio-inspired hierarchical micro- and nano-wrinkles obtained via mechanically directed self-assembly on shape-memory polymers. *Soft Matter* **2017**, *13*, 4328−4334.
(44) Yang, S.; Khare, K.; Lin, P.-C. Harnessing Surface Wrinkle Patterns in Soft Matter. *Adv. Funct. Mater.* **2010**, *20*, 2550−2564.
(45) Rodríguez-Hernández, J. Wrinkled interfaces: Taking advantage of surface instabilities to pattern polymer surfaces. *Prog. Polym. Sci.* **2015**, *42*, 1−41.
(46) Lee, W.-K.; Engel, C. J.; Huntington, M. D.; Hu, J.; Odom, T. W. Controlled Three-Dimensional Hierarchical Structuring by Memory-Based, Sequential Wrinkling. *Nano Lett.* **2015**, *15*, 5624−5629.
(47) Zhang, Z.; Zhang, T.; Zhang, Y. W.; Kim, K.-S.; Gao, H. Strain-Controlled Switching of Hierarchically Wrinkled Surfaces between Superhydrophobicity and Superhydrophilicity. *Langmuir* **2012**, *28*, 2753−2760.
(48) Lee, S. G.; Lee, D. Y.; Lim, H. S.; Lee, D. H.; Lee, S.; Cho, K. Switchable Transparency and Wetting of Elastomeric Smart Windows. *Adv. Mater.* **2010**, *22*, 5013−5017.
(49) Kim, Y. H.; Lee, Y. M.; Lee, J. Y.; Ko, M. J.; Yoo, P. J. Hierarchical Nanoflake Surface Driven by Spontaneous Wrinkling of Polyelectrolyte/Metal Complexed Films. *ACS Nano* **2012**, *6*, 1082−1093.
(50) Wen, G.; Guo, Z.; Liu, W. Biomimetic polymeric superhydrophobic surfaces and nanostructures: from fabrication to applications. *Nanoscale* **2017**, *9*, 3338−3366.
(51) Wu, D.; Sun, J.; Liu, Y.; Yang, Z.; Xu, H.; Zheng, X.; Gou, P. Rapid fabrication of microstructure on PMMA substrate by the plate to plate Transition-Spanning isothermal hot embossing method nearby glass transition temperature. *Polym. Eng. Sci.* **2017**, *57*, 268−274.
(52) Sun, J.; Wu, D.; Liu, Y.; Dai, L.; Jiang, C. Numerical simulation and experimental study of filling process of micro prism by isothermal hot embossing in solid-like state. *Adv. Polym. Technol.* **2017**, 1581−1591.
(53) Yang, Z.-g.; Awuti, G.; Cao, Y.; Zhu, J.; Wu, B.; Wang, J.; Lu, W.; Zhang, X.; Zhang, Q. Preparation and physicochemical characterization of quercetin-HP-beta-CD inclusion complexes. *J. Chin. Pharm. Sci.* **2006**, *15*, 69.
(54) Sun, J.; Zhuang, J.; Jiang, H.; Huang, Y.; Zheng, X.; Liu, Y.; Wu, D. Thermal dissipation performance of metal-polymer composite heat exchanger with V-shape microgrooves: A numerical and experimental study. *Appl. Therm. Eng.* **2017**, *121*, 492−500.
(55) Zhuang, J.; Hu, W.; Fan, Y.; Sun, J.; He, X.; Xu, H.; Huang, Y.; Wu, D. Fabrication and testing of metal/polymer microstructure heat exchangers based on micro embossed molding method. *Microsyst. Technol.* **2018**, 1−8.
(56) Jingyao, S.; Daming, W.; Ying, L.; Zhenzhou, Y.; Pengsheng, G. Rapid fabrication of micro structure on polypropylene by plate to plate isothermal hot embossing method. *Polym. Eng. Sci.* **2018**, *58*, 952−960.
(57) Song, J.; Xie, J.; Li, C.; Lu, J.-h.; Meng, Q.-f.; Yang, Z.; Lee, R. J.; Wang, D.; Teng, L.-s. Near infrared spectroscopic (NIRS) analysis of drug-loading rate and particle size of risperidone microspheres by improved chemometric model. *Int. J. Pharm.* **2014**, *472*, 296−303.
(58) He, X.; Huang, Y.; Liu, Y.; Zheng, X.; Kormakov, S.; Sun, J.; Zhuang, J.; Gao, X.; Wu, D. Improved thermal conductivity of polydimethylsiloxane/short carbon fiber composites prepared by spatial confining forced network assembly. *J. Mater. Sci.* **2018**, *53*, 14299−14310.

DOI: 10.1021/acsomega.8b03138
ACS Omega 2019, 4, 2750−2757